The Seaman Volcanic Center—A Rare Middle Tertiary Stratovolcano in Southern Nevada

U.S. GEOLOGICAL SURVEY BULLETIN 2052

AVAILABILITY OF BOOKS AND MAPS OF THE U.S. GEOLOGICAL SURVEY

Instructions on ordering publications of the U.S. Geological Survey, along with the last offerings, are given in the current-year issues of the monthly catalog "New Publications of the U.S. Geological Survey." Prices of available U.S. Geological Survey publications released prior to the current year are listed in the most recent annual "Price and Availability List." Publications that are listed in various U.S. Geological Survey catalogs (**see back inside cover**) but not listed in the most recent annual "Price and Availability List" are no longer available.

Prices of reports released to the open files are given in the listing "U.S. Geological Survey Open-File Reports," updated monthly, which is for sale in microfiche from the USGS ESIC-Open-File Report Sales, Box 25286, Building 810, Denver Federal Center, Denver, CO 80225

Order U.S. Geological Survey publications **by mail** or **over the counter** from the offices given below.

BY MAIL

Books

Professional Papers, Bulletins, Water-Supply Papers, Techniques of Water-Resources Investigations, Circulars, publications of general interest (such as leaflets, pamphlets, booklets), single copies of periodicals (Earthquakes & Volcanoes, Preliminary Determination of Epicenters), and some miscellaneous reports, including some of the foregoing series that have gone out of print at the Superintendent of Documents, are obtainable by mail from

USGS Map Distribution
Box 25286, Building 810
Denver Federal Center
Denver, CO 80225

Subscriptions to periodicals (Earthquakes & Volcanoes and Preliminary Determination of Epicenters) can be obtained ONLY from

Superintendent of Documents
U.S. Government Printing Office
Washington, DC 20402

(Check or money order must be payable to Superintendent of Documents.)

Maps

For maps, address mail order to

USGS Map Distribution
Box 25286, Building 810
Denver Federal Center
Denver, CO 80225

Residents of Alaska may order maps from

U.S. Geological Survey, Map Sales
101 Twelfth Ave., Box 12
Fairbanks, AK 99701

OVER THE COUNTER

Books

Books of the U.S. Geological Survey are available over the counter at the following U.S. Geological Survey offices, all of which are authorized agents of the Superintendent of Documents.

- **ANCHORAGE, Alaska**–4230 University Dr., Rm. 101
- **ANCHORAGE, Alaska**–605 West 4th Ave., Rm G-84
- **DENVER, Colorado**–Federal Bldg., Rm. 169, 1961 Stout St.
- **LAKEWOOD, Colorado**–Federal Center, Bldg. 810
- **MENLO PARK, California**–Bldg. 3, Rm. 3128, 345 Middlefield Rd.
- **RESTON, Virginia**–National Center, Rm. 1C402, 12201 Sunrise Valley Dr.
- **SALT LAKE CITY, Utah**–Federal Bldg., Rm. 8105, 125 South State St.
- **SPOKANE, Washington**–U.S. Courthouse, Rm. 678, West 920 Riverside Ave.
- **WASHINGTON, D.C.**–U.S. Department of the Interior Bldg., Rm. 2650, 1849 C St., NW.

Maps

Maps may be purchased over the counter at the U.S. Geological Survey offices where books are sold (all addresses in above list) and at the following Geological Survey offices:

- **ROLLA, Missouri**–1400 Independence Rd.
- **FAIRBANKS, Alaska**–New Federal Building, 101 Twelfth Ave.

The Seaman Volcanic Center—A Rare Middle Tertiary Stratovolcano in Southern Nevada

By EDWARD A. DU BRAY

U.S. GEOLOGICAL SURVEY BULLETIN 2052

Geology and geochemical evolution of a rare, well-preserved middle Tertiary stratovolcano

UNITED STATES GOVERNMENT PRINTING OFFICE, WASHINGTON : 1993

U.S. DEPARTMENT OF THE INTERIOR
BRUCE BABBITT, Secretary

U.S. GEOLOGICAL SURVEY
Dallas L. Peck, Director

For sale by
USGS Map Distribution
Box 25286, Building 810
Denver Federal Center
Denver, CO 80225

Library of Congress Cataloging-in-Publication Data

Du Bray, E. A.
The Seaman volcanic center ; a rare middle Tertiary stratovolcano in southern Nevada / by Edward A. du Bray.
p. cm. — (U.S. Geological Survey bulletin ; 2052)
Includes bibliographical references.
Supt. of Docs. no.: I.19.3:B2052
1. Volcanoes—Nevada—Lincoln County. 2. Geology, Stratigraphic—Tertiary. 3. Geochemistry—Nevada—Lincoln County. I. U.S. Geological Survey. II. Title. III. Series.
QE75.B9 no. 2052
[QE524]
557.3 s—dc20
[551.2'1'0979314]

93-2837
CIP

CONTENTS

FIGURES

TABLES

THE SEAMAN VOLCANIC CENTER—A RARE MIDDLE TERTIARY STRATOVOLCANO IN SOUTHERN NEVADA

By EDWARD A. DU BRAY

ABSTRACT

The Seaman volcanic center is a composite, middle Tertiary stratovolcano in southern Nevada; it is about 10 km (6 mi) in diameter and has a reconstructed volume of about 20 km^3 (5 mi^3). The center is principally composed of interbedded dacite lava and pyroclastic flows whose eruption built a stratovolcano that was intruded by rhyolite of a hypabyssal core plug and its associated radial dike.

Almost continuous chemical variation, from the oldest to youngest components of the center, is consistent with periodic tapping of a magma chamber whose contents became progressively more evolved by fractionation, through sidewall crystallization, of observed phenocryst phases. Major- and trace-element abundance variation and covariation groupings, mixing-model calculations, and rare earth element patterns indicate derivation of magma represented by the core plug and radial dike by fractionation and accumulation of hypersthene, calcic plagioclase, hornblende, biotite, apatite, and magnetite from magma represented by the lava flows. The presence of phenocrysts and glomerocrysts composed of various phenocryst combinations indicates that the phases noted above were on the liquidus and accumulating in crystal-rich zones within the chamber.

The development of a stratovolcano in the southern Great Basin, an area in which middle Tertiary volcanism was dominated by ash-flow eruption from caldera sources, may result from a number of factors. As indicated by the scarcity of hydrous silicate phases, particularly in the flow rocks, stratovolcano construction may indicate development of a small chamber that contained relatively volatile poor magma. Older rocks that host the volcanic center contain a relatively low density of intersecting faults. The absence of structural features conducive to ash-flow caldera formation may also have favored stratovolcano formation. Finally, the volume of the Seaman volcanic center is an order of magnitude less than that characteristic of ash-flow caldera-forming systems.

INTRODUCTION

The Seaman volcanic center is clearly denoted as a small, circular volcanic feature on the geologic map of Nevada (Stewart and Carlson, 1978). The west-central part of the Seaman Range is dominated by the Seaman volcanic center (fig. 1), a feature first noted and described by Tschanz and Pampeyan (1961, 1970) and believed by D.C. Noble (University of Nevada–Reno, written commun., 1967, 1970, and 1971, to Ekren and others, 1977) to be a partially eroded composite stratovolcano. Information presented here confirms that the Seaman volcanic center is a middle Tertiary stratovolcano whose gross morphology is remarkably well preserved.

The Seaman volcanic center, about 200 km (125 mi) north of Las Vegas in Lincoln County, Nevada, has a midpoint near lat 37°55' N., long 115°09' W. Ekren and others (1977) suggested that the Seaman volcanic center was active in late Oligocene and early Miocene time. Its age is bracketed between the ages of the underlying Lund Formation (27.9 Ma; Best and Grant, 1987) and overlying rhyolite tuff of the Seaman Range (26.0–27.4 Ma; Ekren and others, 1977, and Taylor and others, 1989). Rocks of the Seaman volcanic center are overlain by the oldest (unit 1 of du Bray and Hurtubise, in press) of the rhyolite tuffs of the Seaman Range. Taylor and others (1989, fig. 8) portrayed the tuff of Hamilton Spring, in the adjacent (to the east) North Pahroc Range, in a stratigraphic position similar to that of unit 1 of the rhyolite tuffs of the Seaman Range; Taylor and Bartley (1988) presented an age of 27.4 Ma for the tuff of Hamilton Spring. Assuming that the tuff of Hamilton Spring is coeval with unit 1 of the rhyolite tuffs of the Seaman Range, development of the Seaman volcanic center is restricted to the period between 27.9 and 27.4 Ma.

The extent to which the Seaman volcanic center was inundated and buried, perhaps completely covered, by younger, onlapping volcanic rocks is unknown; however, the remarkable morphologic preservation of this middle

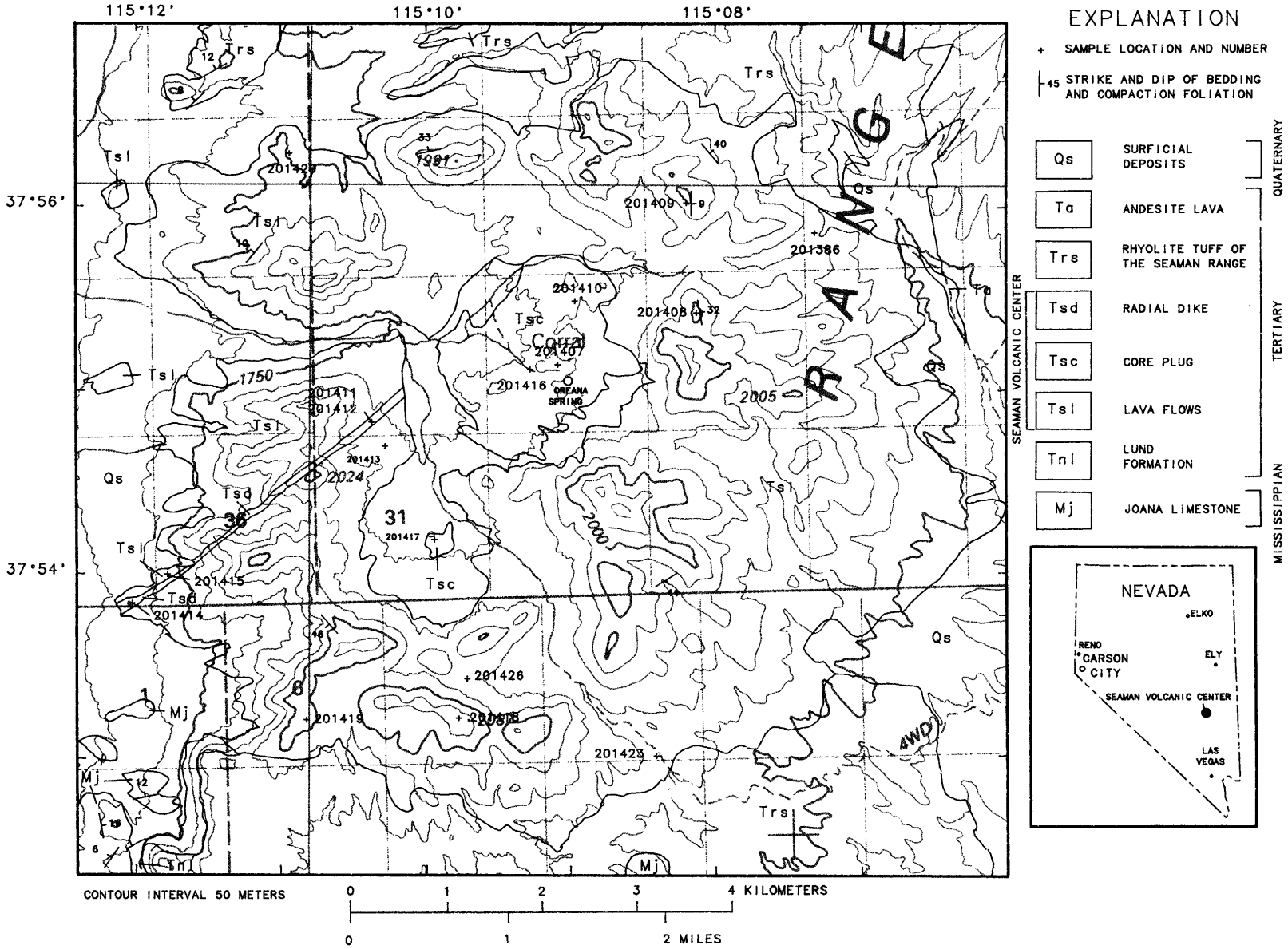

Figure 1. Generalized geologic map of the Seaman volcanic center, Lincoln County, Nevada. Six-digit numbers beginning with 201 indicate sampling sites for samples with geochemical data (tables 1–4).

Tertiary stratovolcano implies that it may have been completely covered and protected from dissection by slightly younger volcanic rocks. Miocene to Pliocene Basin and Range block faulting and subsequent erosion have stripped onlapping rocks from the flanks of the stratovolcano and exhumed it. The core of the volcanic center has been deeply dissected, and the core plug is exposed.

The development of an isolated stratovolcano in this part of the Great Basin, during a period dominated by ash-flow caldera volcanism (Best, Christiansen, and others, 1989, figs. 3, 7), is unusual. Best, Christiansen, and others (1989, p. 93) noted that "Cenozoic lavas are widely scattered throughout the Great Basin* * *lavas occur as isolated domes and flows within a sequence of ash-flow deposits" and that "In contrast to the more or less contemporaneous San Juan volcanic field* * *large constructional volcanoes and associated volcanic debris flows (lahars) are absent in most Great Basin eruptive centers."

Ekren and others (1977) suggested that rhyolitic ash-flow tuff at Hancock Summit, 58 km (36 mi) to the southwest, and tuffaceous rocks to the north and northwest in the Golden Gate Range and to the north in the southern Egan Range are derived from the Seaman volcanic center. His correlations are implausible, however, for a number of reasons. Deposits presumed to be derived from the Seaman volcanic center could have travelled to these relatively distant sites only as ash flows of the type derived from caldera-forming eruptions. Evidence of caldera-forming eruptions associated with the Seaman volcanic center is absent, and far-travelled ash flows are unlikely to have been produced by a stratovolcano. Ash-flow deposits presumed to be derived from the Seaman volcanic center should be preserved, at least locally, even if in very thin layers in the Seaman Range; however, all of the ash flows preserved in the Seaman Range either are from known sources unrelated to the volcanic center or are compositionally (E.A. du Bray, unpub. data, 1992) and petrographically (Hurtubise and du Bray, in press, table 3) dissimilar to components of the volcanic center. It is unlikely that deposits presumed to be derived from the Seaman volcanic center are present in surrounding ranges because deposits related to the center are not known in the Seaman Range, exclusive of the center itself. For these reasons, the correlation offered by Ekren and others (1977) is not valid.

Acknowledgments.—The work reported on here is an outgrowth of the mineral resource assessment of the U.S. Bureau of Land Management Weepah Spring wilderness study area. The author is particularly indebted to J.S. Pallister and G.B. Sidder, whose incisive reviews dramatically improved this report. In addition, G.P. Meeker is thanked for assistance rendered in obtaining electron microprobe mineral chemistry data and M.W. Bultman is thanked for determining densities of samples.

GEOLOGY OF THE SEAMAN VOLCANIC CENTER

The Seaman volcanic center is about 10 km (6 mi) in diameter. Its components include an accumulation, as much as 250 m (820 ft) thick, of lava flows and associated lahars and interbedded pumiceous pyroclastic flows, a hypabyssal core plug approximately 2 km (1.2 mi) in diameter, and a radial dike 50 m (165 ft) wide and approximately 4 km (2.5 mi) long.

The volume of material erupted from the Seaman volcanic center is probably between 15 and 20 km^3 (3.6–4.8 mi^3). These estimates are the result of computing the volume of a cone having dimensions similar to those of the Seaman volcanic center. A volume of 15 km^3 was computed for a cone whose top is truncated (to represent the present-day height of the volcano), whereas a volume of 20 km^3 was computed for a cone whose top was reconstructed by upward extrapolation of the stratovolcano flanks. By analogy to the high-level apophyses inferred by Sillitoe (1973) to intrude the bases of stratovolcanoes that develop above porphyry copper systems, the unexposed part of the solidified core plug in the Seaman volcanic center is considered to have a volume of at most several cubic kilometers.

The igneous products of the Seaman volcanic center range in composition from andesite (minor) to dacite (major) to rhyolite (minor). Andesite to dacite lava flows dip radially away from the central part of the volcanic center and form prominent cliffs. Associated lahars are composed of many varicolored, poorly sorted, bouldery, and pumiceous debris flows. Lahar deposits are especially voluminous on the western flank of the volcanic center in cliffs north of the westward-flowing drainage heading at Oreana Spring (fig. 1). The hypabyssal core plug is weakly hydrothermally altered in some places and weathers to bouldery outcrops. The dike, also affected by weak deuteric alteration in some places, forms prominent castellated outcrops along its 4 km (2.5 mi) length. The dike and core plug intrude, and therefore are younger than, the lava flows; because the contact between the dike and plug is not exposed, age relations between the dike and plug are unknown.

The volcanic center is in one of the least deformed parts of the Seaman Range. Evidence that might indicate localization of the volcanic center by major structural features is absent, although rocks of the Seaman volcanic center probably conceal some older faults (Hurtubise and du Bray, 1992).

PETROGRAPHY

Lavas erupted from the Seaman volcanic center are light-brownish-gray to dark-gray dacite that forms

prominent cliffs composed of radially outward dipping flows. The dacite contains about 10 percent crystals. Phenocrysts (fig. 2*A*), in decreasing order of abundance, are subhedral, strongly (oscillatory) zoned plagioclase (0.2–4 mm), subhedral hypersthene (0.2–3 mm), trace amounts of anhedral to subhedral magnetite (0.1 mm), and anhedral quartz (2 mm), and accessory allanite, apatite (abundant as minute inclusions in hypersthene, fig. 2*B*), and rare oxyhornblende in a pilotaxitic, devitrified-glass groundmass that contains plagioclase microlites. Glomerocrysts composed of plagioclase, hypersthene, and magnetite are a characteristic feature of the dacite lava flows (fig. 2*C*); trace amounts of brown interstitial glass are present in some glomerocrysts. The lava flow unit (fig. 1) also contains massively bedded, varicolored, poorly sorted, bouldery lahars and (or) block and ash pyroclastic flow deposits; groundmass is ash and contains abundant pumice blocks 1–5 cm in diameter.

The core plug consists of light-greenish-gray to light-brownish-gray, fine-grained, porphyritic, hypabyssal rhyolite and dacite that weathers to rounded boulders and outcrops. The plug contains about 8 percent crystals. Phenocrysts, in decreasing order of abundance, are subhedral zoned plagioclase (1.5–3 mm), subhedral hornblende laths altered to biotite (0.5–2 mm), and trace amounts of anhedral, resorbed and embayed quartz (2–4 mm), subhedral biotite (1–1.5 mm), subhedral hypersthene (0.5–1 mm), and anhedral magnetite (0.1 mm) in a fine-grained groundmass of quartz and feldspar (fig. 2*D*). Plagioclase glomerocrysts are present in some samples of the core plug.

The radial dike is grayish-black to light-yellowish-gray and light-gray, porphyritic rhyolite to dacite. The dike is inhomogeneous with respect to petrographic and compositional characteristics along its length and across its width, and it is enclosed in a distinctive black-glass chilled margin several meters thick. The dike contains about 10 percent crystals. Phenocrysts, in decreasing order of abundance, are subhedral zoned plagioclase (0.5–4 mm), anhedral sanidine (1–8 mm), anhedral, deeply embayed quartz (1–3 mm), subhedral hornblende (0.5 mm), subhedral hypersthene (0.2–0.4 mm), and trace amounts of subhedral biotite (0.1–1 mm) and anhedral magnetite (0.1 mm) in a devitrified-glass groundmass that contains feldspar microlites (fig. 2*E*).

Phenocrysts in some Seaman volcanic center samples have textures that imply phenocryst-melt disequilibrium; others show the effects of deuteric alteration. The rims of most pyroxene crystals (as well as cores in some cases) in samples of the lava flows are altered to opaque masses of fine-grained iron-titanium oxide minerals. Hornblende laths in many samples of the core plug have been replaced by biotite. Crystals that form some glomerocrysts show disequilibrium textures; a second generation of plagioclase rims primary grains whose cores are altered to sericite, and pyroxene crystals are almost uniformly replaced by felted, opaque intergrowths of iron-titanium oxide minerals.

GEOCHEMISTRY OF THE SEAMAN VOLCANIC CENTER

WHOLE-ROCK CHEMISTRY

All of the geochemical data presented here were determined in analytical laboratories of the U.S. Geological Survey in Denver, Colorado. Major-oxide analyses (table 1) were performed (analysts, J.E. Taggart, A.J. Bartel, and K. Stewart) using X-ray fluorescence techniques (Taggart and others, 1987). FeO:FeO* (total iron as FeO) molar ratios were adjusted to 0.85 and major-oxide abundances recalculated to 100 percent, on an anhydrous basis. Trace element abundances in table 2 were determined (by du Bray) by energy-dispersive X-ray fluorescence spectroscopy (Elsass and du Bray, 1982) using ^{109}Cd and ^{241}Am radioisotope excitation sources; the accuracy of this type of data is discussed by Sawyer and Sargent (1989). Trace element data in table 3 were determined (analyst, J.R. Budahn) by instrumental neutron activation analysis (INAA) (Baedecker and McKown, 1987).

Trace element data obtained by X-ray fluorescence spectroscopy were used to identify the range of compositional variation for seventeen samples of Seaman volcanic center components. A representative subset of nine samples was selected in order to depict the range of major element variation of components of the volcanic center. Similarly, the least evolved lava sample, the most evolved dike sample, and a representative sample of the core plug were selected for instrumental neutron activation analysis.

The system of the International Union of Geological Sciences (Le Bas and others, 1986) was used to classify the rocks of the Seaman volcanic center (table 1, fig. 3). The lava flows range in composition from andesite to dacite although most of the flows are dacite. The core plug and the radial dike are transitional from dacite to rhyolite. The core plug and radial dike contain 0–0.19 (average 0.05, table 4) and 0.30–1.57 (average 0.99, table 4) percent normative corundum (table 1), respectively.

All components of the Seaman volcanic center are subalkaline (fig. 3) and contain roughly equal amounts of Na_2O and K_2O. Average Na_2O+K_2O values (table 4) are 5.90, 6.98, and 7.00 at SiO_2 values of 65.4, 70.6, and 70.5, respectively, for the lava flows, central plug, and radial dike (all in weight percent, normalized to 100 percent, anhydrous). Compositions of components of the Seaman volcanic center plot near the Cascade calc-alkaline trend on an AFM (Na_2O+K_2O-FeO-MgO) diagram (fig. 4) and are within the calc-alkaline field as defined by Irvine and Baragar (1971).

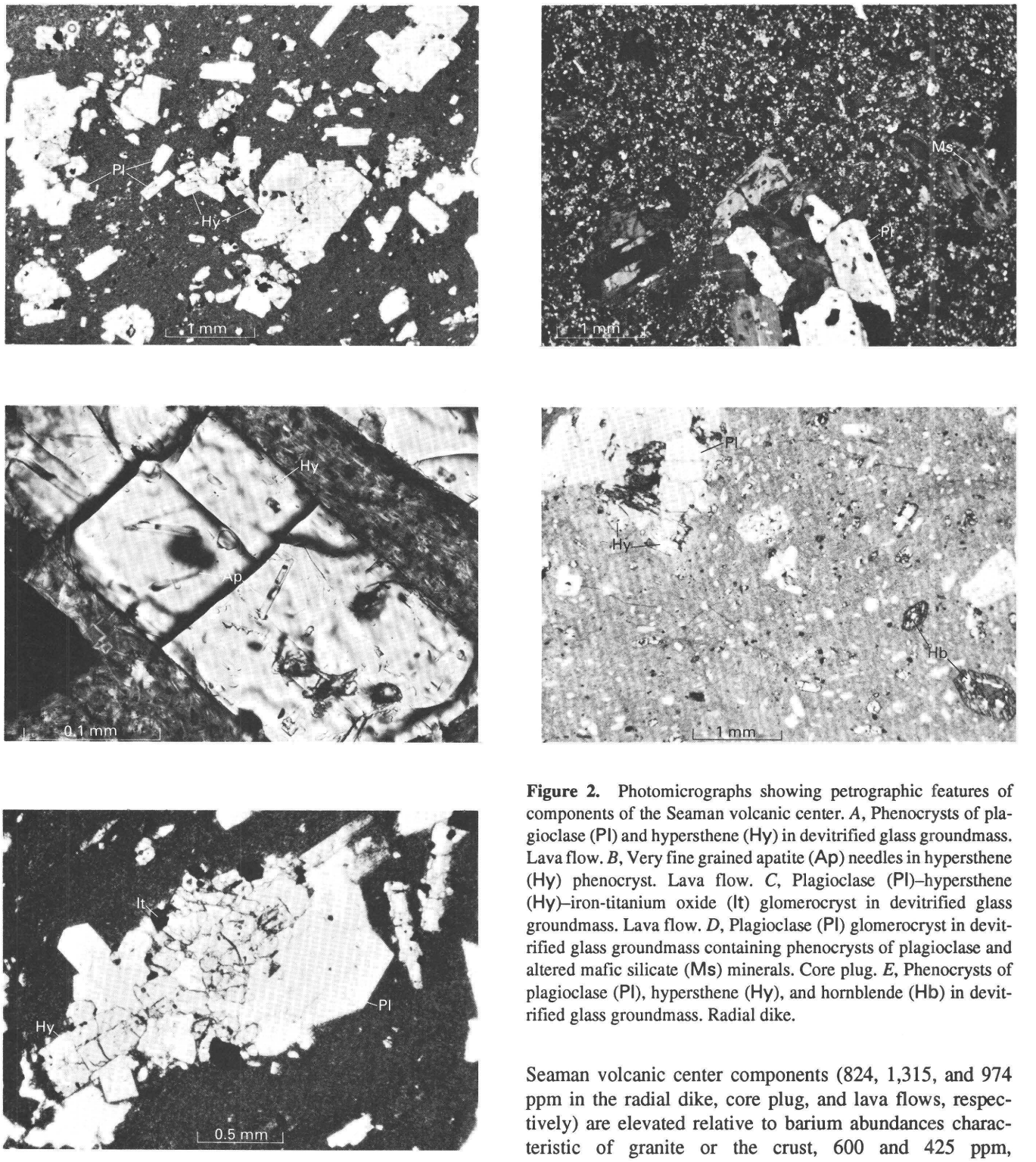

Figure 2. Photomicrographs showing petrographic features of components of the Seaman volcanic center. *A*, Phenocrysts of plagioclase (Pl) and hypersthene (Hy) in devitrified glass groundmass. Lava flow. *B*, Very fine grained apatite (Ap) needles in hypersthene (Hy) phenocryst. Lava flow. *C*, Plagioclase (Pl)–hypersthene (Hy)–iron-titanium oxide (It) glomerocryst in devitrified glass groundmass. Lava flow. *D*, Plagioclase (Pl) glomerocryst in devitrified glass groundmass containing phenocrysts of plagioclase and altered mafic silicate (Ms) minerals. Core plug. *E*, Phenocrysts of plagioclase (Pl), hypersthene (Hy), and hornblende (Hb) in devitrified glass groundmass. Radial dike.

Abundances for most trace elements in components of the Seaman volcanic center (tables 2, 3) are within ranges characteristic of calc-alkaline, middle Tertiary volcanic rocks of the Basin and Range province (Best, Christiansen, and Blank, 1989). Average barium abundances in Seaman volcanic center components (824, 1,315, and 974 ppm in the radial dike, core plug, and lava flows, respectively) are elevated relative to barium abundances characteristic of granite or the crust, 600 and 425 ppm, respectively (Krauskopf, 1979). Rb/Sr ratios range from a low value of 0.21 in the lava flows to a more evolved value of 0.56 in the radial dike (table 4). Rubidium and strontium abundances vary systematically from the oldest (elevated strontium and depleted rubidium) to the youngest (depleted strontium and elevated rubidium) components of the Seaman volcanic center (fig. 5). Note,

Table 1. Major-oxide and CIPW normative mineral composition for samples of the Seaman volcanic center, Lincoln County, Nevada.
[Major oxide data normalized to 100 weight percent, anhydrous; LOI, loss on ignition; Fe^{2+}:Fe^{3+} set to 0.8; Sum_0, original analytical total; $FeTO_3$, analytical value for total iron as Fe_2O_3. Leaders (--), not present]

Unit	Radial dike			Core plug			Lava flows		
Sample No.	201411	201412	201414	201407	201410	201417	201409	201415	201423
Major-oxide composition									
SiO_2	68.84	69.84	72.84	70.62	71.13	70.04	68.81	64.87	62.55
Al_2O_3	15.81	15.96	14.36	14.99	14.84	14.93	15.22	16.88	17.32
Fe_2O_3	0.54	0.49	0.37	0.46	0.46	0.55	0.62	0.88	1.03
FeO	2.74	2.52	1.90	2.35	2.33	2.83	3.16	4.48	5.23
MgO	1.03	.54	.58	.83	.61	.95	1.04	1.14	1.68
CaO	3.67	3.06	2.04	3.19	2.91	3.52	3.65	4.89	5.94
Na_2O	3.55	3.09	2.87	3.01	3.07	3.13	3.11	3.45	2.94
K_2O	3.08	3.78	4.64	4.05	4.19	3.48	3.74	2.54	2.22
TiO_2	.55	.56	.27	.37	.34	.42	.48	.58	0.76
P_2O_5	.14	.15	.08	.10	.09	.10	.11	.18	.21
MnO	.06	.01	.04	.03	.04	.04	.06	.10	.11
LOI	1.83	2.62	2.14	1.75	1.53	2.17	1.05	1.66	1.53
Sum_0	100.19	99.38	99.83	99.43	99.49	99.57	99.93	99.88	100.27
$FeTO_3$	3.51	3.18	2.43	2.99	2.97	3.59	4.07	5.73	6.72
CIPW normative mineral composition									
Q	25.69	28.95	32.09	28.28	28.81	28.05	25.44	20.39	18.92
C	0.30	1.57	1.10	0.09	0.19	--	--	0.01	--
or	18.19	22.35	27.40	23.96	24.73	20.57	22.13	15.00	13.12
ab	30.03	26.13	24.30	25.45	25.98	26.49	26.28	29.18	24.91
an	17.28	14.22	9.59	15.16	13.82	16.41	16.54	23.06	27.48
hy	6.35	4.66	4.28	5.45	4.95	6.31	6.83	9.56	11.65
di	--	--	--	--	--	.33	0.72	--	0.49
mt	.78	0.72	0.54	.67	.66	0.80	.90	1.27	1.49
il	1.05	1.06	.51	.70	.64	.80	.91	1.11	1.45
ap	.34	.34	.19	.24	.22	.24	.26	.44	.51

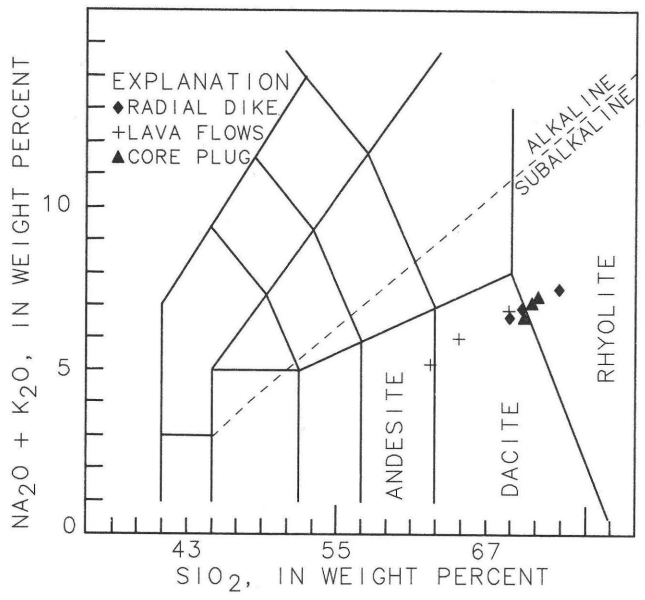

Figure 3. Alkali-silica classification diagram (Le Bas and others, 1986) showing analyses (table 1) of samples from the Seaman volcanic center. Alkaline-subalkaline dividing line from Irvine and Baragar (1971).

however, the continuous variation of rubidium and strontium abundances between components of the Seaman volcanic center and the overlap between abundances of these two elements between at least one of the lava flow samples and some core plug and radial dike samples.

Chondrite-normalized rare earth element patterns for samples of the Seaman volcanic center have a gentle negative slope and small to very small negative europium anomalies (fig. 6). Patterns for lava flow and radial dike samples are almost parallel, whereas a core plug sample has a crossing pattern; it is light rare earth element enriched and heavy rare earth element depleted relative to the lava and dike samples. The magnitude of the europium anomaly increases from the lava flows and core plug to the radial dike. Light- and heavy-rare earth element abundances are about 100 and 10 times chondritic values, respectively; $(La/Lu)_N$ values are 6.7 and 15.5 in lava flow and core plug samples, respectively. Total rare earth element contents range from 127 (radial dike) to 157 (core plug and lava flow) ppm. The relatively less evolved (with respect to SiO_2 abundances and Rb-Sr ratios, for instance) lava flows have rare earth element contents that are

Table 2. Trace element data for samples of the Seaman volcanic center, Lincoln County, Nevada.
[In parts per million]

Unit	Radial dike			Core plug				Lava flows	
Sample No.	201411	201412	201414	201407	201410	201416	201417	201386	201408
Rb	127	137	177	128	128	118	108	80	78
Sr	326	262	200	380	326	372	366	434	414
Y	22	25	23	20	19	18	21	39	28
Zr	163	162	135	153	148	148	175	233	208
Nb	13	14	15	11	12	13	11	15	15
Ba	876	796	800	1,327	1,366	1,242	1,326	930	793
La	34	31	35	47	41	42	54	34	40
Ce	58	58	65	73	82	64	90	69	68
Nd	31	32	34	42	36	30	34	36	37

Unit	Lava flows							
Sample No.	201409	201413	201415	201418	201419	201423	201426	201429
Rb	108	91	58	84	93	66	73	122
Sr	387	457	446	388	385	437	401	344
Y	20	27	27	32	27	35	28	19
Zr	154	187	190	195	191	214	205	147
Nb	11	13	14	13	15	12	12	10
Ba	1,201	996	1,008	905	927	880	833	1,268
La	40	36	34	43	39	32	38	45
Ce	65	67	68	74	71	67	70	69
Nd	35	30	30	34	29	34	34	34

Table 3. Instrumental neutron activation data for samples of the Seaman volcanic center, Lincoln County, Nevada.
[In parts per million. bdl, below detection limit]

Unit	Radial dike	Core plug	Lava flows
Sample No.	201414	201407	201423
Ba	804	1,360	886
Co	4.39	3.98	10.9
Ni	8.2	6.2	bdl
Cr	10.3	8.82	18.3
Cs	6.23	3.21	1.79
Hf	4.20	4.25	5.27
Rb	181	124	57.3
Sb	0.310	0.150	0.237
Ta	2.71	0.985	0.820
Th	15.1	12.8	7.65
U	5.80	4.11	2.03
Zn	60.3	57.3	104
Zr	117	147	180
Sc	5.37	7.61	18.7
La	31.2	38.8	33.6
Ce	58.1	74.3	70.6
Nd	24.5	30.6	32.7
Sm	5.55	5.49	6.77
Eu	.792	1.18	1.56
Gd	4.32	4.42	6.42
Tb	0.607	0.580	0.931
Tm	bdl	0.293	0.534
Yb	1.82	1.78	3.43
Lu	0.270	0.260	0.519

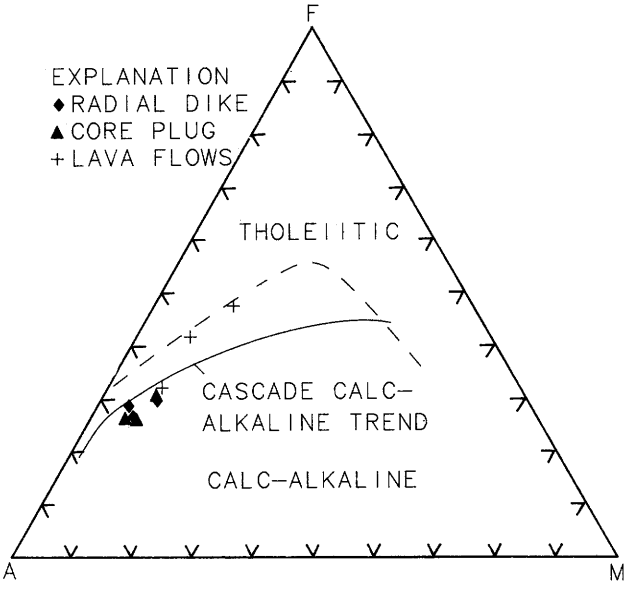

Figure 4. Ternary AFM (Na_2O+K_2O-FeO^*-MgO) diagram showing compositions of samples from the Seaman volcanic center. Cascade calc-alkaline trend (solid line) and tholeiitic–calc-alkaline (dashed line) dividing lines from Irvine and Baragar (1971).

Table 4. Average major-oxide, CIPW normative, and trace-element compositions of components of the Seaman volcanic center, Lincoln county, Nevada.

[*n*, number of analyses from which mean and standard deviation were calculated. Major-oxide and CIPW normative data in weight percent, normalized to 100 percent, anhydrous; LOI, loss on ignition; trace element data in parts per million; leaders (--), not detected; ±, calculated standard deviation]

	Radial dike *n*=3	Core plug *n*=3	Lava flows *n*=3
Major-oxide composition			
SiO_2	70.50±2.08	70.59±0.55	65.41±3.17
Al_2O_3	15.38±0.88	14.92±0.07	16.47±1.11
Fe_2O_3	0.47±0.08	0.49±0.06	0.84±0.21
FeO	2.39±0.43	2.50±0.28	4.29±1.05
MgO	0.72±0.27	0.80±0.17	1.28±0.35
CaO	2.92±0.82	3.21±0.31	4.83±1.14
Na_2O	3.17±0.35	3.07±0.06	3.17±0.26
K_2O	3.83±0.78	3.91±0.37	2.83±0.80
TiO_2	0.46±0.17	0.38±0.04	0.61±0.15
P_2O_5	0.12±0.04	0.10±0.01	0.17±0.05
MnO	0.04±0.03	0.03±0.04	0.09±0.03
LOI	2.20±0.40	1.82±0.33	1.41±0.32
CIPW normative mineral composition			
Q	28.91	28.36	21.58
C	0.99	0.05	--
or	22.65	23.09	16.75
ab	26.82	25.97	26.79
an	13.70	15.26	22.37
hy	5.10	5.61	9.35
di	--	--	0.40
mt	0.68	0.71	1.22
il	0.87	0.72	1.15
ap	0.29	0.24	0.40
Trace element composition			
	n=3	*n*=4	*n*=10
Rb	147±27	121±10	85±19
Sr	263±63	361±24	409±31
Y	23±2	20±1	28±6
Zr	153±16	156±13	190±31
Nb	14±1	12±1	13±2
Ba	824±45	1,315±52	974±153
La	33±2	46±6	38±4
Ce	60±4	77±11	69±3
Nd	32±2	36±5	33±3

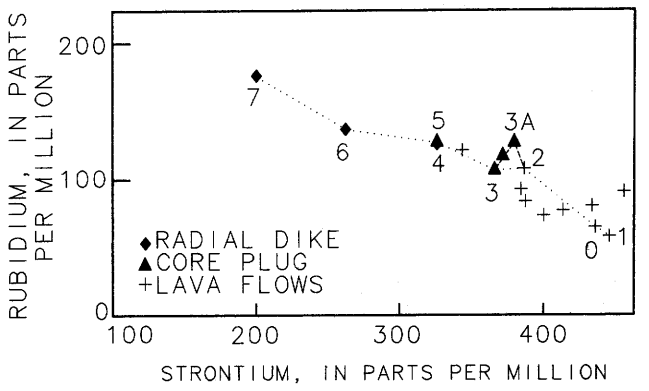

Figure 5. Diagram showing the variation of rubidium and strontium abundances in samples from the Seaman volcanic center. Lines connect sample points whose major oxide compositions were evaluated in mixing model calculations (table 5). Numbers next to points depict the sequence, starting with 1 and ending with 6, in which compositions were derived in mixing calculations; point 0 depicts the sample whose composition was designated as that of the most primitive liquid in this system. Numbers followed by the letter A indicate alternate liquid evolution paths, as described in text.

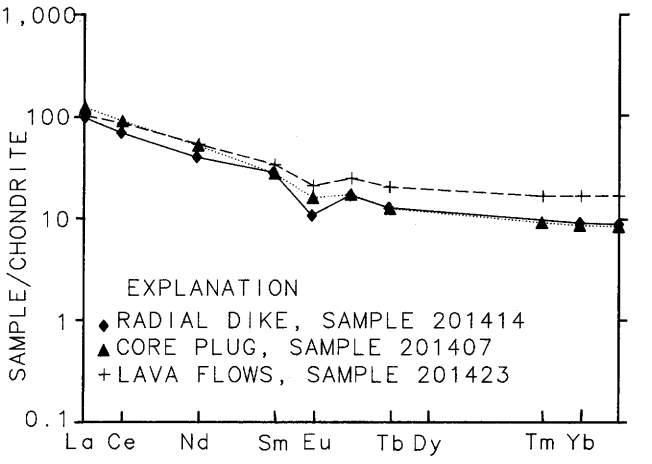

Figure 6. Chondrite (Anders and Ebihara, 1982)-normalized diagram showing compositions (table 3) of samples from the Seaman volcanic center.

systematically greater than those of the more evolved radial dike.

Spidergrams (Thompson and others, 1983) (fig. 7) facilitate comparison of incompatible trace element abundances in components of the Seaman volcanic center. Patterns are relatively smooth (with superimposed negative Ba, Nb, Ta, Sr, P, and Ti anomalies) and have a gentle negative slope. Normalized abundances are from about 600 to 9 times chondritic values. Chondrite-normalized patterns for the radial dike and lava flow are the most and least, respectively, negatively sloping. The radial dike is characterized by the most well developed negative anomalies.

Compositional data for each of the components of the Seaman volcanic center are characterized by groups of oxides and elements whose abundances display mutual covariation. Abundances of total iron, TiO_2, CaO, Al_2O_3, MgO, P_2O_5, MnO, Sr, Zr, and Y and of SiO_2, K_2O, Rb, and Ba vary systematically. These covariance relations suggest that compositional variation within the Seaman components is controlled by observed phenocryst phases.

In samples of each of the three Seaman components, total iron, TiO_2, and CaO abundances are strongly correlated; correlation coefficients (*r*) exceed 0.9. Abundances of MgO are also correlated with this group of elements. In

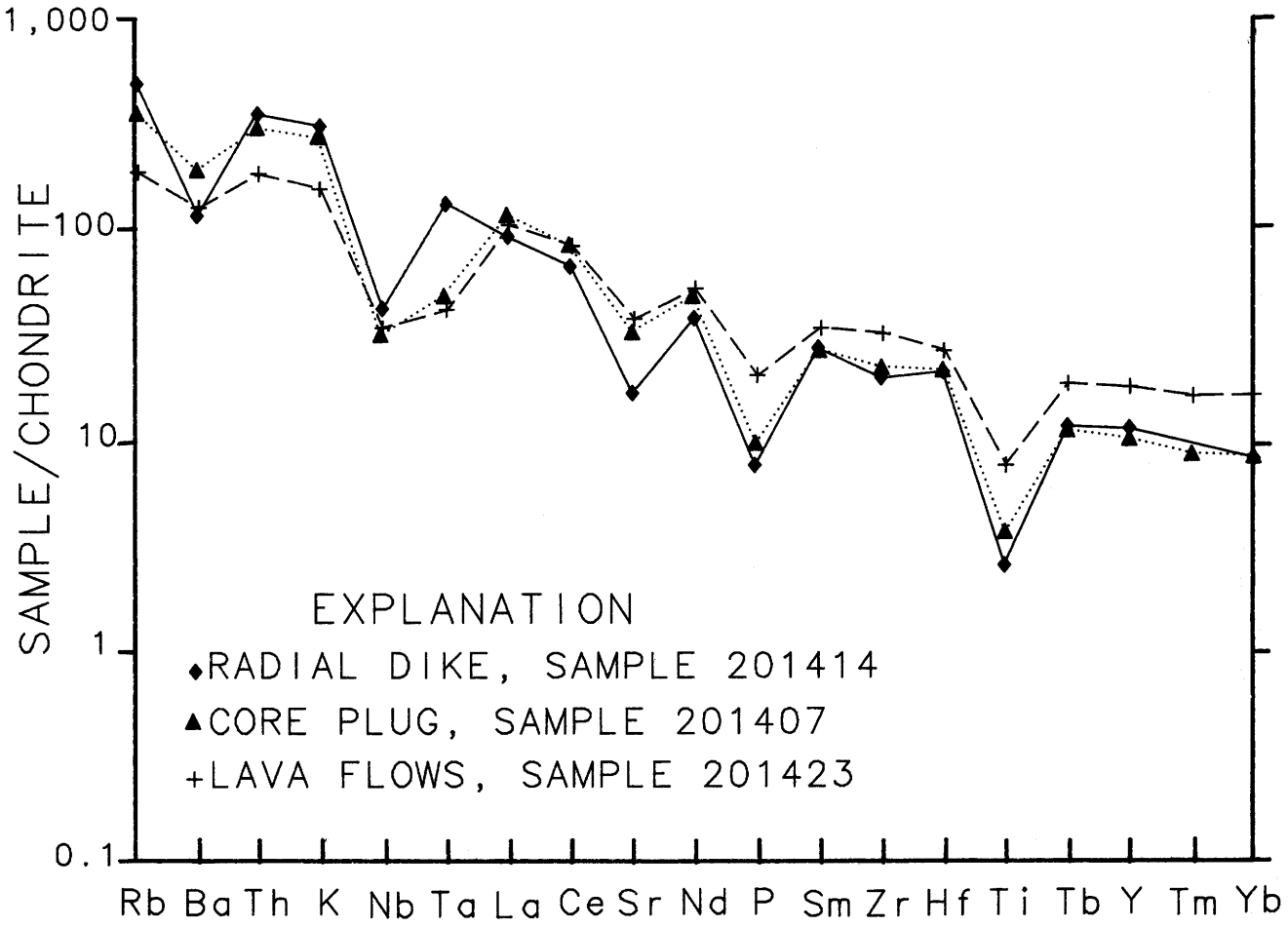

Figure 7. Chondrite (Thompson and others, 1983)-normalized extended trace element diagram showing compositions (tables 1–3) of samples from the Seaman volcanic center. Trace elements are arranged in order of increasing compatibility to the right.

samples of the core pluton and lava flows, *r* values for MgO and these elements exceed 0.9 (except total iron in core pluton samples, 0.79). In samples of the radial dike, *r* values for MgO and these elements exceed 0.6 (except TiO_2, *r* is 0.4). Abundances of Al_2O_3 and P_2O_5 in samples of the radial dike and of the lava flows are also strongly correlated (*r* exceeds 0.95) with total iron, TiO_2, and CaO abundances. In samples of the lava flows, MnO abundances display strong covariance (*r* exceeds 0.88) with all of the oxides (except MgO, *r* is 0.75) mentioned above. Abundances of strontium, yttrium, and zirconium vary systematically with abundances of most of the oxides described above (*r* exceeds 0.8 in most cases), though abundances of yttrium in radial dike samples do not exhibit this behavior.

In samples of each of the three components of the Seaman volcanic center, abundances of K_2O, SiO_2, and rubidium have *r* values in excess of 0.95; barium joins this group in samples of lava flows. In samples of the radial dike, abundances of K_2O, SiO_2, and rubidium co-vary as do those of Na_2O, CaO, barium, and strontium (*r* exceeds 0.85, except CaO and barium is 0.76).

Major-oxide and trace-element covariance relations discussed above may reflect control by fractionation and (or) accumulation of hypersthene, calcic plagioclase, hornblende, biotite, apatite, and magnetite. The compositions of hypersthene ($[Mg,Fe]SiO_3$) and hornblende ($[Na,K]$-$Ca_2[Mg,Fe,Al]_5[Si_6Al_2][OH,F]_2$) are appropriate to control total iron, MgO, zirconium, and yttrium and some CaO and MnO abundance variations in components of the Seaman volcanic center. Hypersthene in Seaman rocks contains distinctive, accessory amounts of apatite, which controls P_2O_5, strontium, and some of the CaO abundance variations. Zirconium and yttrium are inferred to occur as trace constituents, substituting for other cations, in hypersthene and hornblende; likewise strontium is inferred to substitute for calcium in apatite. The fact that yttrium and other oxides of the total iron-TiO_2-CaO-Al_2O_3-MgO-P_2O_5-MnO group do not display systematic covariation in dike samples suggests that yttrium was partitioned into a phase (an iron-titanium oxide mineral or unidentified trace mineral) other than hypersthene or hornblende during evolution of the magma represented by the radial dike. MgO covariations in dike samples suggest that the abundance of

Table 5. Representative mineral compositions for phenocryst phases in samples of the Seaman volcanic center, Lincoln County, Nevada.

[*n*, number of analyses from which mean and standard deviation were calculated; leaders (--), not detected; H_2O in hornblende and biotite determined by difference]

Sample no.	Plagioclase		Hypersthene		Hornblende	Biotite
	201386	201413	201386	201413	201413	201410
	n=6	*n*=8	*n*=9	*n*=6	*n*=6	*n*=4
Mineral composition						
SiO_2	45.94±0.50	48.80±0.60	50.21±0.34	50.32±0.25	41.63±0.34	36.34±1.44
Al_2O_3	33.94±0.27	32.06±0.51	0.45±0.06	0.76±0.20	10.90±0.28	13.32±1.13
FeO	0.18±0.04	0.23±0.03	30.85±0.98	29.84±0.92	19.51±0.34	17.24±1.82
MgO	--	--	14.79±0.77	16.00±0.82	9.05±0.15	13.26±1.62
CaO	17.45±0.47	15.25±0.51	1.66±0.09	1.46±0.07	10.69±0.07	--
Na_2O	1.38±0.19	2.75±0.30	--	--	2.29±0.49	0.20±0.10
K_2O	0.04±0.01	.08±0.02	--	--	0.76±0.04	8.91±0.26
TiO_2	--	--	0.17±0.07	0.11±0.06	2.55±0.08	3.81±0.51
MnO	--	--	0.68±0.06	0.66±0.06	0.19±0.03	0.15±0.03
H_2O	--	--	--	--	2.43±0.28	6.78±0.27
Sum	98.93	99.16	98.80	99.15	100.00	100.00
Structural formula						
No. oxygens	32		6		24	24
Si	8.542	8.999	1.986	1.972	6.299	5.624
Al	7.439	6.969	0.014	0.028	1.701	2.376
Al	--	--	0.007	0.007	0.243	0.056
Ti	--	--	0.005	0.003	0.290	0.443
Fe^{+2}	0.029	0.035	1.021	0.978	2.470	2.231
Mn	--	--	0.023	0.022	0.025	0.019
Mg	--	--	0.872	0.935	2.041	3.058
Ca	3.476	3.013	0.070	0.061	1.733	--
Na	0.498	0.983	--	--	0.672	0.059
K	0.009	0.019	--	--	0.147	1.760
OH	--	--	--	--	2.460	6.596
Site occupancy						
Z	15.981	15.968	2.000	2.000	8.000	8.000
Y	--	--	1.928	1.945	2.552	5.807
X	4.012	4.050	0.070	0.061	5.069	1.819
End-member mineral proportions						
Ab	12.5	24.5	Wo	3.6	3.1	
An	87.3	75.0	En	44.4	47.4	
Or	0.2	0.5	Fs	52.0	49.5	

MgO may have been controlled by a phase, possibly biotite, other than hypersthene or hornblende. In lava flow samples, strong abundance covariation between MnO and other oxides discussed above suggests that MnO was principally sited in hypersthene or hornblende in the lava flows but in some other phase (again perhaps biotite) in the other two Seaman volcanic center components. The K_2O, SiO_2, rubidium, and barium abundance covariance relations discussed above are considered to reflect fractionation and (or) accumulation of biotite, whereas calcic plagioclase controls Na_2O, CaO, barium, and strontium abundance variations. Rubidium, barium, and strontium are inferred to be present as trace constituents, substituting for potassium and sodium in plagioclase and biotite, as appropriate.

MINERAL CHEMISTRY

Mineral compositions (table 5) were determined using an ARL SEMQ electron microprobe equipped with six wavelength dispersive spectrometers. A 20-micron beam was used to analyze phenocrysts. Sample current was 15 nA (on brass), and accelerating voltage was 15 kV. Natural and synthetic materials were used as standards. Compositions were determined for least three points distributed across the width of at least two grains per mineral species during 20-second analyses.

The average compositions of plagioclase in samples 201386 and 201413 (table 5) are statistically distinct and are calcium-rich and calcium-poor bytownite, respectively. The plagioclase within each of these samples is

compositionally zoned; grain cores are calcium rich and sodium poor relative to grain rims. Compositional zonation spans 5–10 mol percent in the anorthite component.

The compositions of orthopyroxene in samples 201386 and 201413 (table 5) are very similar. The compositions of these phenocrysts plot in the ferrohypersthene field of Deer and others (1966). Core to rim zonation is much less pronounced in pyroxenes of the Seaman volcanic center than in plagioclase; zonation of several percent in the enstatite and ferrosalaite end members was identified.

The composition of hornblende in sample 201413 (table 5) is distinct in that its TiO_2 and Na_2O+K_2O contents are elevated relative to those of common hornblende. These features and the fact that this amphibole contains subequal cationic amounts of iron and magnesium are consistent with its having an affinity to kaersutitic amphibole. The low standard deviations associated with the mean oxide abundances calculated from six analyses (two analysis points for each of three grains) indicates that these phenocrysts are relatively compositionally homogeneous.

The composition of mica in sample 201410 (table 5) is that of a slightly magnesium enriched biotite (Foster, 1960). Similar to the hornblende in sample 201413, the biotite in sample 201410 is somewhat titanium enriched. Moderate standard deviations associated with the mean oxide abundances calculated from four analyses (two analysis points for each of two grains) indicate that these phenocrysts are somewhat compositionally inhomogeneous. Slightly low (relative to mica analyses; Deer and others, 1966), analytical totals and somewhat elevated calculated (by difference) H_2O contents for these micas imply that they have been affected by weak deuteric or hydrothermal alteration, in accord with petrographic observations.

MAJOR ELEMENT LEAST-SQUARES FRACTIONATION-MIXING MODELING

In order to more rigorously evaluate the role of phenocryst fractionation or accumulation in the compositional evolution of the Seaman volcanic center, major element least-squares crystal fractionation-mixing models were calculated using PETMIX IV (Kevin W. Laurent, U.S. Geological Survey, unpub. software, version 2.1b). The sequential derivation of progressively more evolved major-oxide compositions (table 1) by fractionation of phenocrysts having compositions like those determined in samples of Seaman components (table 5) is evaluated in table 6.

Numerical input to the modeling process was modified and selected somewhat from that presented in tables 1 and 5. All iron in whole-rock and mineral compositions was recalculated to the ferrous state. The compositions of plagioclase and hypersthene from two lava flow samples (201386 and 201413) were utilized in the modeling process. Hypersthene and plagioclase compositions in sample 201386 are considerably more primitive (higher FeO and CaO, respectively) than those in sample 201413 and were used as fractionation-mixing phases only in the first modeling increment. Plagioclase and pyroxene were used throughout the modeling process, which is in accord with their occurrence as phenocrysts in all samples of Seaman volcanic center components. Hornblende and biotite compositions (table 5) determined for phenocrysts in samples 201413 and 201410, respectively, were used in modeling steps 3–7, which is in accord with the absence of these phases in samples represented by the first two modeling steps. Magnetite and apatite, present in all samples of Seaman components, were used throughout the modeling process; their compositions were selected from Colucci and others (1991, analysis HMM 130 OX8) and Deer and others (1966, apatite analysis no. 1), respectively, because the compositions of these phases are relatively constant.

The numerical modeling process allows minerals to be subtracted or added during least-squares calculations. Numerical output from the modeling process indicating that a mineral was subtracted to drive computed liquid compositions toward the model endpoint identifies a phase that crystallized and was mechanically separated (fractionated) from the residual liquid. Numerical output indicating that a mineral was added indicates a mineral that was mechanically added to the residual liquid.

The physical process of crystal fractionation is logical and intuitive, whereas the process for crystal addition is not. Components of the Seaman volcanic center are characterized by the presence of glomerocrysts, which indicate that crystallization was occurring in the chamber. The physical process of crystal addition, suggested by output from the modeling process (table 6, numerical entries preceded by a +), involves recombination (by convective stirring) of crystals nucleated in one part of the chamber with residual magma from another part of the chamber.

The results of major element least-squares crystal fractionation-mixing modeling are considered meaningful when the quantity Σr^2 (table 6), the sum of the squares of the residuals for each of the evaluated major element components, is less than the value ascribed to analytical uncertainty (approximately 0.5–1.0 weight percent) for the analyses being modeled. Values of Σr^2 greater than 1.0 indicate that the proposed model has not addressed petrologic processes or components operative in the genesis of the compositions being evaluated.

The value of Σr^2 is less than 0.35 in six of nine models for the Seaman volcanic center and is less than 0.15 in four of these. Consequently, models calculated for sequential derivation of the Seaman components by

Table 6. Results of major element least-squares crystal fractionation-mixing modeling for samples of the Seaman volcanic center, Lincoln County, Nevada.

[Entries in "Step" column refer to incremental episodes modeled along the inferred fractionation path, compare with figure 5. Numbers under mineral headings are mass percentages of each phase removed (or, if preceded by a plus sign (+), added) in each fractionation step; F, mass percent of derived liquid composition relative to parent liquid]

			Plagioclase		Hypersthene				Hornblende	Biotite		
Step	Parent	Derived	201386	201413	201386	201413	Magnetite	Apatite	201413	201410	F	Σr^2
1	201423	201415	7.69	--	4.82	--	0.06	0.31	--	--	87.12	0.1053
2	201415	201409	--	12.62	--	1.79	1.76	0.10	--	--	83.92	0.6480
3A	201409	201407	--	3.64	--	1.57	0.77	0.17	--	--	93.84	0.0568
3	201407	201417	--	+1.69	--	+1.92	+0.09	0.18	+3.40	3.38	103.53	0.0670
	or											
3	201409	201417	--	0.60	--	+2.28	0.55	0.11	0.63	2.93	97.45	0.0160
4	201417	201411	--	+4.45	--	0.98	0.08	0.29	+1.01	+1.02	105.27	0.4683
5	201411	201410	--	7.54	--	2.18	+0.32	+0.45	4.74	+2.24	88.55	0.7592
6	201410	201412	--	+7.01	--	+1.12	+0.89	0.20	4.55	+1.14	105.42	0.2251
7	201412	201414	--	9.31	--	+0.34	1.07	+0.24	1.57	+0.71	89.34	0.3123

fractionation-mixing are valid. The three highest Σr^2 values are 0.7592, 0.6480, and 0.4683 for derivation of compositions represented by samples 201410, 201409, and 201411, respectively. In all of these cases the major contributions to elevated Σr^2 values involve large residuals, of opposite sign, for Na_2O and K_2O. These components are notoriously mobile in glassy volcanic rocks and are easily redistributed by circulating hydrothermal fluids or during devitrification and hydration (Lipman, 1965). All three of these samples show signs of weak alteration or glassy groundmass devitrification. The high residuals for these three models probably reflect an alkali remobilization component not addressed by the calculated model. Consequently, the results of calculations involving these three samples are more meaningful than the Σr^2 values indicate.

The sequence in which compositions were incrementally modeled was primarily determined by evaluation of rubidium versus strontium abundances (fig. 5). Variations in the relative abundances of these two elements are a reliable indicator of degree of geochemical behavior because rubidium is incompatible in most intermediate-composition igneous systems and strontium is compatible (Hanson, 1980). Therefore, of the nine samples of the Seaman volcanic center for which major element data are available the two samples having the highest strontium and lowest rubidium abundances were initially selected as potential starting points for the fractionation-mixing modeling. In turn, the sample having the next highest rubidium and next lowest strontium abundances was identified as the starting point for the next composition increment to be modeled. This pattern was continued until the sample having the second highest rubidium and second lowest strontium abundances was used to model derivation of the most evolved sample by fractionation-mixing of observed phenocryst phases.

The rubidium and strontium abundances of the two potential starting point samples (201415 and 201423, table 2) are indistinguishable within analytical precision (Sawyer and Sargent, 1989), but the abundances (table 1) of the more refractory major element components (including total iron, MgO, CaO, and TiO_2) are distinctly higher in sample 201423. Consequently, the composition of sample 201423 was selected as that from which to begin fractionation-mixing modeling.

Similarly, although the rubidium and strontium abundances of samples 201410 and 201411 are indistinguishable, the more refractory major element components are distinctly higher in sample 201411; accordingly, the modeling sequence was constructed such that the composition of sample 201411 was derived from that of sample 201417 and was used as the starting point for derivation of the composition of sample 201410.

Two paths were modeled between major element compositions for samples 201409, 201407, and 201417 (paths 3 and 3A, fig. 5, table 6). The rubidium and strontium abundances for sample 201407 do not plot near the trend exhibited by the compositions for the remainder of the modeled sample compositions. Consequently, an alternate path from the composition of sample 201409 to that of sample 201417, skipping the composition of sample 201407 was modeled. Both paths are characterized by very low values of Σr^2 and neither path is obviously more meaningful.

EVOLUTION OF THE SEAMAN VOLCANIC CENTER

Field relations indicate that the Seaman volcanic center is a composite stratovolcano that developed by episodic lava flow eruption and by emplacement of associated pyroclastic flows and lahars; final magmatic activity at the Seaman volcanic center is denoted by the hypabyssal core plug and associated radial dike, both of which intruded the earlier erupted products. The Seaman

volcanic center was constructed between about 27.9 and 27.4 Ma, between emplacement of the underlying Lund Formation and the oldest of the overlying ash-flow tuffs of the Seaman Range. Significantly larger stratovolcanoes have developed in considerably shorter time periods. Mount Shasta in northern California, for instance, has a volume 20 times greater than that of the Seaman volcanic center and developed in 0.35 m.y. (Christiansen and Miller, 1989). The 0.5 m.y. available for development of the Seaman volcanic center is therefore more than ample.

The thick section of lahars and pyroclastic flows in the northwestern part of the Seaman volcanic center fills a large topographic depression in the lava flow sequence. These deposits indicate that lava interacted with water during at least the waning stages of lava flow eruption. The large volume of lahars, together with their coarseness and lack of sorting, indicates rapid deposition and incorporation of a large volume of water, possibly in the form of snowpack or glacial ice. The bedded character of the lahars and the lack of voluminous debris flow deposits in the area immediately surrounding the Seaman volcanic center argue against a sector collapse origin for these deposits. The three-dimensional shape and large volume of the lahar deposits indicate that the northwestern flank of the stratovolcano was breached during or after emplacement of the lava flows; the breaching process was probably directly linked to the processes responsible for lahar generation.

The radial dike probably represents extraction of the final, most evolved fraction of Seaman magma and emplacement into a local, northeast-trending fracture. The orientation of the fracture that controlled localization of the radial dike may have been influenced by the prevailing regional stress field; fracture development probably began during solidification of the core plug. Delaney and others (1986) indicated that in the general case the orientation of dike-hosting fractures is "perpendicular to the direction of least compressive regional stress acting at the time of dike emplacement." Taylor and Bartley (1988) and du Bray and Hurtubise (in press) showed that normal faults active in nearby areas immediately prior to development of the Seaman volcanic center are oriented northeast to north-northeast, a direction that implies the least principal stress direction was oriented northwest to west-northwest. In accord with theoretical predictions, the northeast-trending radial dike of the Seaman volcanic center was emplaced in a fracture that is perpendicular to the direction of the least compressive regional stress.

Volatile phase exsolution results in a net volume expansion (Burnham and Ohmoto, 1980), which imposes stress on overlying rocks. Crystallization of magma represented by the core plug may have resulted in volatile saturation, fluid phase exsolution, and consequent volume expansion. Hence, lava flows of the Seaman volcanic center were fractured in the direction perpendicular to the minimum regional stress direction by volume expansion in the underlying, solidifying reservoir. The resulting fracture served as a conduit for magma represented by the radial dike.

Major-oxide and trace-element compositions of the components of the Seaman volcanic center indicate that progressively more evolved magmas were erupted during evolution of the stratovolcano (fig. 8). Most notably, abundances of total iron, MgO, CaO, TiO_2, P_2O_5, MnO, and compatible trace elements (including Sr, Co, Cr, Zn, and Sc) are highest in samples of the lava flows, whereas abundances of SiO_2, total alkalis, and incompatible trace elements (including Rb, Cs, Ta, Th, and U) are highest in samples of the central plug and radial dike (tables 3, 4). Major-oxide abundances vary smoothly and continuously (fig. 5) between the components of the volcanic center, and compositions of some lava flow samples (samples from the highest stratigraphic positions) overlap those of the core plug and radial dike (fig. 3). The youngest lavas have compositions similar to those of the core plug and radial dike; the last fraction of liquid that was erupted was compositionally similar to magma represented by the core plug and radial dike.

It is noteworthy that the last phase of magmatism (represented by the core plug and radial dike) associated with the Seaman volcanic center is the most geochemically evolved. This trend is opposite to that predicted by top-down tapping of a chemically zoned chamber (Hildreth, 1981). Several possibilities for eruption of geochemically primitive magma followed by emplacement of somewhat more evolved magma are considered below.

The reversed chemical zonation may result from a two-stage process. The lava flows could have been erupted so soon after emplacement of magma into an upper crustal magma chamber that development of compositional zonation in the chamber was precluded. After eruption of the lava flows, the residual magma may have differentiated and become compositionally zoned; the more evolved, upper part of the chamber is then represented by the youngest lava flows and by the core plug and the radial dike. This two-stage process would probably result in a compositional discontinuity between the lava flows and subsequent igneous products that is not present in compositional data for the Seaman volcanic center (figs. 3–5). In addition, this two-stage process probably could not generate the volume of lava flows derived from the Seaman volcanic center. The presence of interbedded lava flows, pyroclastic flows, and lahars indicates complex and episodic eruptions over a considerable time span that probably are incompatible with a simple two-stage model.

Alternatively, reversed chemical zonation may result from eruption dynamics prevailing during evacuation of a normally zoned chamber. Very high eruption rates could cause deeper, less evolved parts of the chamber to be

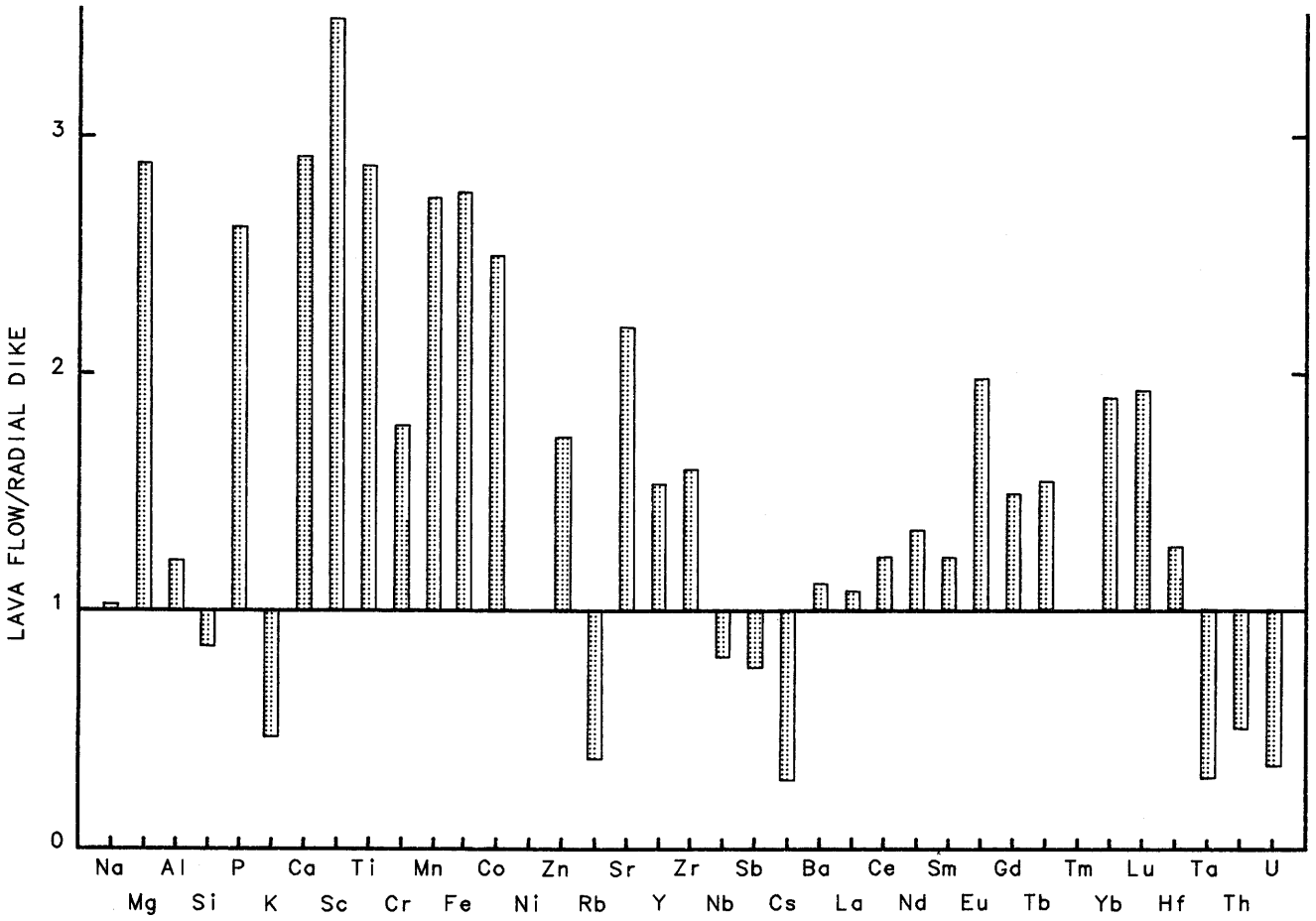

Figure 8. Enrichment-depletion diagram showing major- and trace-element abundances of the Seaman volcanic center dike normalized to those of the lava flow unit.

extracted while more evolved magma in the upper part of the chamber is effectively necked off and prevented from entering eruption conduits. Similar, discontinuously (or reversely) zoned ash-flow tuff deposits derived from Plinian eruptions were considered by Boden (1989) to reflect rapid eruption from a discontinuously (stepwise) zoned chamber. Boden indicated that the subsequent eruption (emplacement) of more evolved material from the same chamber may "reflect eruption of residual silicic layers of magma that restratified below the vent during pauses in the eruptive cycle." However, the eruption rates and dynamics that prevail during Plinian eruptions and during multiple eruptions of lava from a stratovolcano over an extended period of time are different to the extent that the necking-off process is an unlikely explanation for the compositional variation of rocks of the Seaman volcanic center.

The preferred model for eruption and emplacement of progressively more evolved magmas from the Seaman volcanic center involves a variation on the process of sidewall crystallization described by Sawka and others (1990) for zoned plutons of the Sierra Nevada batholith. This solidification model is invoked for magma chambers in which cooling is inferred to proceed from the margin inward by conductive heat loss to host rock forming the chamber walls. As cooling proceeds, mafic silicate minerals, calcic plagioclase, and trace phases crystallize along the chamber walls. Sawka and others (1990) described processes of interstitial liquid migration toward the top of the chamber that may not be applicable to evolution of the Seaman volcanic center. Instead, the melt in the Seaman chamber is inferred to become more evolved by removal of components necessary for sidewall crystallization of these refractory phases. Continuous sidewall crystallization, convective mixing between refractory-component-depleted sidewall melt and undepleted melt inboard from the crystallization front, and periodic tapping of the compositionally evolving, convectively mixed central part of the chamber results in an inward-crystallizing magma chamber characterized by more evolved compositions from the walls inward and eruption of progressively more evolved lavas.

A series of high-level reservoirs above the main chamber may have controlled lava flow eruption. The last

of these reservoirs may be represented by the core plug and radial dike. The progressively more evolved composition of lavas erupted from the Seaman volcanic center and the most evolved compositions of its core plug and radial dike are logical consequences of sidewall crystallization, residual liquid differentiation, and magma emplacement in small, high-level, eruption-producing reservoirs.

Thus, the hypabyssal core plug of the Seaman volcanic center probably represents the top of the final in a series of small volume reservoirs and not a large, solidified, high-level magma chamber that directly fed lava flow eruptions. Initially, these reservoirs probably developed in older rocks (Paleozoic carbonate rocks and Oligocene ash-flow tuff) that host the volcanic center and, ultimately, as the stratovolcano grew in height, in the base of the stratovolcano itself. Sillitoe (1973) depicted bodies such as the core plug of the Seaman volcanic center as apophyses above much larger plutons whose tops are approximately 4 km beneath the stratovolcano base. Similarly, Pallister and others (1992) indicated that juvenile material for the 1980 eruption of Mount St. Helens was supplied from a small reservoir whose top was about 7 km below the 1980 crater floor. By analogy, the core plug of the Seaman volcanic center may represent the solidified equivalent of the last, high-level reservoir from which lava flows were erupted. Eruption from this reservoir probably ceased following eruption of the youngest lava flows when magma supply from the underlying chamber diminished. With an end to effusive activity the volcanic center became inactive and the final reservoir solidified to the core plug.

Sparse gravity data (du Bray and others, 1987, fig. 3) indicate a broad, low-amplitude high associated with the area of the Seaman volcanic center. Dacite lava flows and the core plug of the center are more dense (2.51 and 2.61 g/cm^3, respectively, E.A. du Bray, unpub. data, 1992) than the thin accumulation of dacite to rhyolite ash-flow tuff (1.4–2.5 g/cm^3, average about 2.1 g/cm^3; Cook, 1965, and Williams, 1967) exposed at the surface in this area but are significantly less dense than the thick section of carbonate sedimentary rocks (2.6–2.8 g/cm^3; Dobrin, 1976, p. 455–456) in the shallow subsurface throughout the Seaman Range (du Bray and others, 1987, p. E7). Taken together, these features suggest that a pluton, the solidified magma chamber that periodically supplied the series of small, high-level reservoirs beneath the evolving stratovolcano and is more dense than its host Paleozoic carbonate rocks, is present beneath the Seaman volcanic center.

The density (greater than 2.8 g/cm^3) required for the inferred pluton to have an associated gravity anomaly high relative to the enclosing Paleozoic carbonate rocks indicates a quartz diorite to gabbro composition (Dobrin, 1976). Such a pluton represents the refractory, early crystallized, relatively more dense part of a solidified magma chamber that was periodically tapped to supply the series of high-level reservoirs. The composition of magma in these reservoirs, and thus the composition of the erupted products, would have become progressively more evolved with time as a result of crystallization and fractionation in the underlying source chamber.

With the exception of the core plug and radial dike, hypabyssal to exogenous volcanic features such as those that intruded lava flows on the flanks of stratovolcanoes of the modern Cascades volcanic arc, including Mount Mazama (Bacon, 1983) and Mount St. Helens (Crandell, 1987), are not exposed in the deeply incised flanks of the Seaman volcanic center. The Seaman volcanic center thus probably evolved entirely by central vent eruption. By analogy to construction of stratovolcanoes of the modern Cascade arc, numerous eruptive episodes were probably required to complete construction of the Seaman volcanic center. Because the core plug and dike are all that remains of the magmatic plumbing system of the Seaman volcanic center, it is likely that successive eruptive episodes obliterated previously developed, central exogenous domes in a manner similar to that which characterized early (May–October 1980) central dacite dome development at Mount St. Helens following its May 1980 eruption (Swanson and others, 1987). The solidified, unerupted contents of high-level reservoirs inferred to have preceded that represented by the central plug may form stocks in the shallow subsurface beneath the Seaman volcanic center.

Rare earth element abundances of the radial dike and core plug, in particular heavy rare earth element abundances, which are depleted relative to those characteristic of the lava flows, are consistent with hypersthene and hornblende fractionation. Mineral-matrix distribution coefficients for hypersthene range from 0.1 to 1.14 (Hanson, 1980), whereas those for hornblende range from 1 to 14. Mineral-matrix rare earth element patterns for hypersthene and hornblende have gentle positive slopes and small negative europium anomalies (Hanson, 1980); heavy rare earth element enrichment in hornblende is maximized at dysprosium or erbium and flattens or tails off in ytterbium and lutetium. Although hypersthene fractionation will cause heavy rare earth elements to be depleted relative to light rare earth elements in the residual melt, its fractionation will not appreciably reduce the rare earth element content of the residual liquid because hypersthene-melt distribution coefficients are less than one in most cases. Consequently, heavy rare earth element abundance reduction between the lava flows and the core plug and radial dike was principally controlled by hornblende fractionation. The cause of light rare earth element depletion of the radial dike relative to the lava flows and core plug is unknown but may reflect late-stage fractionation of a light rare earth element-enriched accessory phase such as allanite or monazite (Miller and Mittlefehldt, 1982).

Abundance variations involving rubidium and strontium indicate that feldspar fractionation was important in compositional evolution of the Seaman volcanic center.

Feldspar-melt distribution coefficients for rubidium and strontium in intermediate composition rocks (Hanson, 1980) indicate that feldspar fractionation preferentially removes strontium relative to rubidium from the melt phase. Feldspar crystallization causes residual liquids (such as those represented by the youngest parts of the Seaman volcanic center, namely the core plug and radial dike) to become progressively rubidium enriched relative to strontium. Europium (fig. 6) and strontium and barium (fig. 7) abundances are most depleted in the most evolved component of the volcanic center (radial dike), which is also consistent with a derivation of the radial dike that involved feldspar fractionation. Similarly, the negative phosphorous and titanium anomalies (fig. 7) are probably a consequence of apatite and iron-titanium oxide fractionation, respectively. Co-nucleation of apatite and hypersthene is indicated by the fact that apatite is included as very fine grained needles within hypersthene phenocrysts. Consequently, apatite and hypersthene fractionation are linked. As hypersthene phenocrysts grew, incorporated minute apatite crystals, and separated from the melt phase, they removed apatite and the components contained therein.

The presence of plagioclase-hypersthene glomerocrysts in most samples of the Seaman volcanic center provides additional, tangible evidence that these phases played an essential role in the chemical evolution of the components of the center. Fractionation-mixing calculations support the inference that varying amounts of plagioclase, hypersthene, hornblende, biotite, apatite, and magnetite fractionation and convective remixing with glomerocrysts controlled compositional evolution of components of the volcanic center. These phases probably crystallized along the walls of the cooling magma chamber, and residual silicate liquid continued convective overturn, mixing, and evolution in the central part of the chamber. Eruption dynamics may have caused some of the sidewall crystal accumulations to be disrupted and mixed back into residual silicate liquids such that they are almost ubiquitously present in components of the volcanic center.

Southward-sweeping, middle Tertiary volcanism in the Basin and Range province is considered to be a consequence of decreasing convergence rate between the Pacific and North American plates, stagnation of shallow subduction along the North American plate margin, subsequent foundering of the subducted Pacific plate, and pronounced asthenospheric backflow beneath the continental lithosphere of western North America (Lipman, 1980; Best and Christiansen, 1991). The Seaman volcanic center is a minor manifestation of this volcanic arc magmatism.

Several trace element characteristics of components of the Seaman volcanic center confirm the inference that the center evolved in a volcanic arc setting. In particular, negative Nb-Ta anomalies (fig. 7) are considered to be a hallmark of magmas generated in a volcanic arc setting (Wood and others, 1979; Gill, 1981). Ba/Ta ratios greater than 450 and La/Nb ratios of 2–7 are also considered to indicate magma genesis in a volcanic arc setting. Ba/Ta ratios are 297, 1,380, and 1,080 in the radial dike, core plug, and lava flows of the Seaman volcanic center, respectively, whereas La/Nb ratios are 2.1, 3.5, and 2.8, respectively.

Pearce and others (1984) recognized that granitic rocks from different settings are characterized by distinctive geochemical signatures, and they developed trace element discriminant diagrams to infer tectonic setting. Trace element abundance variations in coeval volcanic and plutonic rocks from any given terrane should be similar. Consequently, the tectonic setting–trace element discriminant diagrams developed by Pearce and others (1984) are used herein to evaluate the tectonic setting that prevailed during the development of the Seaman volcanic center. Samples from the volcanic center plot in the volcanic arc field on these diagrams (fig. 9), consistent with development of the center in a volcanic arc setting and with the regionally based inference that the Basin and Range province was a volcanic arc terrane during middle Tertiary time.

The existence of the isolated Seaman stratovolcano in a region dominated by caldera-style volcanism (Best, Christiansen and others, 1989) is unusual. Several factors, including the volume of the associated magma chamber, the volatile content of contained magma, and the structural setting, may have caused the Seaman volcanic center to develop as a stratovolcano rather than as an ash-flow caldera.

The small volume of the Seaman volcanic center is outside the range of values characteristic of caldera-forming ash-flow eruptions. Smith (1979) indicated that large, epicontinental caldera-forming eruptions involve magma volumes of 100–1,000 km^3, whereas eruptions with volumes of 1–100 km^3 form stratovolcanoes and small epicontinental ring structures. The total volume (exposed plus inferred volume of unexposed core plug) of the Seaman volcanic center is only about 20 km^3, at the low end of the stratovolcano–small ring structure range. The volume of magma emplaced into the Seaman volcanic center chamber was probably insufficient to initiate the processes that drive and sustain ash-flow caldera-style eruptions.

Magmatic volatile saturation and the rapid vesiculation that occurs when a magma is depressurized are essential to initiation of ash-flow eruptions (Smith, 1979). Relatively low inferred magma volatile contents may have contributed to the style of eruption at the Seaman volcanic center. Primary hydrous silicate minerals (hornblende and biotite), whose nucleation indicates relatively volatile rich magma, are almost absent from lava flow samples of the Seaman volcanic center and are not abundant in samples of the core plug. Samples of the lava flows and core plug contain rare phenocrysts of hornblende, whereas some samples of the core plug contain biotite phenocrysts; most

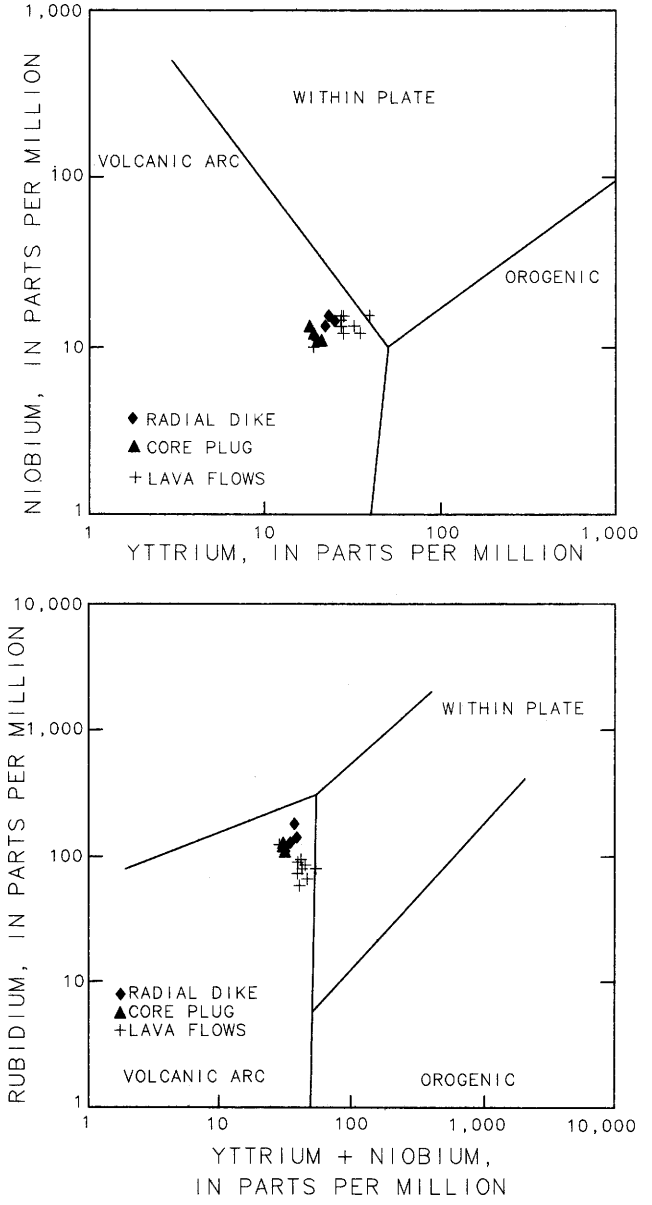

Figure 9. Tectonic setting–trace element discriminant variation diagrams for components of the Seaman volcanic center; abundances expressed in parts per million. Tectonic setting–composition boundaries from Pearce and others (1984). *A*, Rubidium versus yttrium plus niobium. *B*, Niobium versus yttrium.

contain phenocrysts of pyroxene and lesser amounts of hornblende.

Volatile contents (LOI, tables 1, 4) of components of the Seaman volcanic center are low and may corroborate the inference, from the scarcity of hydrous phenocryst phases, that magmas of the Seaman volcanic center were relatively volatile poor. It is important to note, however, that measured volatile abundances in fresh volcanic rocks are typically less than magmatic abundances because volatile components are lost through exsolution and outgassing accompanying and following eruption. Analyzed volatile contents may, however, be greater than magmatic values due to hydration that accompanies glassy groundmass devitrification. The best estimates of pre-eruption volatile contents are derived from analysis of glass inclusions; no glass inclusions have been identified in samples of the Seaman volcanic center. The lava flows, core plug, and radial dike contain 1.41, 1.82 and 2.20 weight percent volatile constituents, respectively (LOI, table 4).

Estimated magmatic volatile contents, which provide an indication of volatile contents necessary for initiation of ash-flow eruptions, are summarized by Whitney (1988). These estimates range from 2.2 (Bishop Tuff) to 4.0 (Fish Canyon Tuff) weight percent H_2O. Relatively elevated volatile abundances probably did not develop in the chamber of the Seaman volcanic center until late in its evolution. The volatile abundances in magmas of the center were probably too low to initiate an ash-flow caldera-forming eruption.

The structural setting in the rocks that host the Seaman volcanic center also may have inhibited the rapid vesiculation necessary for the onset of a caldera-forming eruption. A densely faulted and fractured terrane is more likely to experience catastrophic failure, leading to spontaneous depressurization and vesiculation in an underlying magma chamber, than a geologically coherent terrane. The density of intersecting faults in older rocks exposed peripheral to the Seaman volcanic center is low (du Bray and Hurtubise, in press), with the result that the host rocks of the center confined the center to a relatively coherent eruption style.

SUMMARY AND CONCLUSIONS

The Seaman volcanic center in southern Nevada is a composite, middle Tertiary stratovolcano principally composed of dacite lava flows and interbedded pyroclastic flows and lahars, a hypabyssal core plug, and a radial dike. The volcano developed through initial eruption of lava flows, forming a stratovolcano, and subsequent intrusion and solidification of a core plug and a radial dike. The Seaman volcanic center probably evolved from magma emplaced into a chamber that cooled and solidified from its walls inward. Sidewall crystallization resulted in a refractory-component-depleted residual silicate liquid, which by mixing with undepleted magma caused the composition of undepleted magma in the central part of the chamber to become progressively evolved. Chemical and field relations suggest that the volcanic center erupted progressively more evolved lava flows from a series of small, high-level reservoirs. Geochemical zonation in the chamber of the volcanic center probably resulted primarily from fractionation of plagioclase, hypersthene, and hornblende. The chamber of the Seaman

volcanic center may have formed a stratovolcano instead of a caldera because of its small size, relatively low volatile content, and a structural setting not conducive to development of an ash-flow caldera.

REFERENCES CITED

Anders, Edward, and Ebihara, Mitsuru, 1982, Solar-system abundances of the elements: Geochimica et Cosmochimica Acta, v. 46, p. 2363–2380.

Bacon, C.R., 1983, Eruptive history of Mount Mazama and Crater Lake caldera, Cascade Range, U.S.A.: Journal of Volcanology and Geothermal Research, v. 18, p. 57–115.

Baedecker, P.A, and McKown, D.M., 1987, Instrumental neutron activation analysis of geochemical samples, *in* Baedecker, P.A., ed., Methods for geochemical analysis: U.S. Geological Survey Bulletin 1770, p. H1–H14.

Best, M.G., and Christiansen, E.H., 1991, Limited extension during peak Tertiary volcanism, Great Basin of Nevada and Utah: Journal of Geophysical Research, v. 96, p. 13509–13528.

Best, M.G., Christiansen, E.H., and Blank, H.R., Jr., 1989, Oligocene caldera complex and calc-alkaline tuffs and lavas of the Indian Peak volcanic field, Nevada and Utah: Geological Society of America Bulletin, v. 101, p. 1076–1090.

Best, M.G, Christiansen, E.H., Deino, A.L., Gromm, C.S., McKee, E.H., and Noble, D.C., 1989, Excursion 3A—Eocene through Miocene volcanism in the Great Basin of the western United States, *in* Chapin, C.E., and Zidek, Jiri, eds., Field excursions to volcanic terranes in the Western United States—Cascades and Intermountain West: New Mexico Bureau of Mines and Mineral Resources Memoir 47, v. 2, p. 91–133.

Best, M.G., and Grant, S.K., 1987, Stratigraphy of the volcanic Oligocene Needles Range Group in southwestern Utah and eastern Nevada: U.S. Geological Survey Professional Paper 1433–A, 28 p.

Boden, D.R., 1989, Evidence for step-function zoning of magma and eruptive dynamics, Toquima caldera complex, Nevada: Journal of Volcanology and Geothermal Research, v. 37, p. 39–57.

Burnham, C.W., and Ohmoto, H. 1980, Late-stage processes of felsic magmatism: Mining Geology Special Issue, no. 8, p. 1–11.

Christiansen, R.L., and Miller, C.D., 1989, Mount Shasta and vicinity, *in* Chapin, C.E., and Zidek, Jiri, eds., Field excursions to volcanic terranes in the western United States—Cascades and Intermountain West: New Mexico Bureau of Mines and Mineral Resources Memoir 47, v. 2, p. 216–225.

Colucci, M.T., Dungan, M.A., Ferguson, K.M., Lipman, P.W., and Moorbath, S., 1991, Precaldera lavas of the southeast San Juan volcanic field—Parent magmas and crustal interactions: Journal of Geophysical Research, v. 96, p. 13413–13434.

Cook, E.F., 1965, Stratigraphy of Tertiary volcanic rocks in eastern Nevada: Nevada Bureau of Mines Report 11, 61 p.

Crandell, D.R., 1987, Deposits of pre-1980 pyroclastic flows and lahars from Mount St. Helens volcano, Washington: U.S. Geological Survey Professional Paper 1444, 91 p.

Deer, W.A., Howie, R.A., and Zussman, J., 1966, An introduction to the rock forming minerals: London, Longman, 528 p.

Delaney, P.T., Pollard, D.D., Ziony, J.I., and McKee E.H., 1986, Field relations between dikes and joints—Emplacement processes and paleostress analysis: Journal of Geophysical Research, v. 91, p. 4920–4938.

Dobrin, M.B., 1976, Introduction to geophysical prospecting: New York, McGraw-Hill, 630 p.

du Bray, E.A., Blank, H.R., Jr., Turner, R.L., Gese, D.D., and Harris, A.D., 1987, Mineral resources of the Weepah Spring Wilderness Study Area, Lincoln and Nye Counties, Nevada: U.S. Geological Survey Bulletin 1728, p. E1–E11.

du Bray, E.A., and Hurtubise, D.O., in press, Geologic map of the Seaman Range, Lincoln and Nye Counties, Nevada: U.S. Geological Survey Miscellaneous Investigations Series Map I–2282, scale 1:50,000.

Ekren, E.B., Orkild, P.P., Sargent, K.A., and Dixon, G.L., 1977, Geologic map of Tertiary rocks, Lincoln County, Nevada: U.S. Geological Survey Miscellaneous Investigations Series Map I–1041, scale 1:250,000.

Elsass, Francoise, and du Bray, E.A., 1982, Energy-dispersive X-ray fluorescence spectrometry with the Kevex 7000 system: Saudi Arabian Deputy Ministry Mineral Resources Open-File Report USGS–OF–02–52, 53 p.

Foster, M.D., 1960, Interpretation of the composition of trioctahedral micas: U.S. Geological Survey Professional Paper 354–B, 49 p.

Gill, James, 1981, Orogenic andesites and plate tectonics: New York, Springer-Verlag, 390 p.

Hanson, G.N., 1980, Rare earth elements in petrogenetic studies of igneous systems: Annual Review of Earth and Planetary Sciences, v. 8, p. 371–406.

Hildreth, W., 1981, Gradients in silicic magma chambers—Implications for lithospheric magmatism: Journal of Geophysical Research, ser. B, v. 86, p. 10153–10192.

Hurtubise, D.O., and du Bray, E.A., 1992, Stratigraphy and structure of the Seaman Range and Fox Mountain, Lincoln and Nye Counties, Nevada: U.S. Geological Survey Bulletin 1988–B, 31 p.

Irvine, T.N., and Baragar, W.R.A., 1971, A guide to the chemical classification of the common volcanic rocks: Canadian Journal of Earth Sciences, v. 8, p. 523–548.

Krauskopf, K.B., 1979, Introduction to geochemistry (2nd ed.): New York, McGraw-Hill, 721 p.

Le Bas, M.J., Le Maitre, R.W., Streckeisen, A., and Zannetin, B., 1986, A chemical classification of volcanic rocks based on the total alkali-silica diagram: Journal of Petrology, v. 27, p. 745–750.

Lipman, P.W., 1965, Chemical comparison of glassy and crystalline volcanic rocks: U.S. Geological Survey Bulletin 1201–D, p. D1–D24.

———1980, Cenozoic volcanism in the western United States—Implications for continental tectonics, in Continental tectonics: National Academy of Sciences, p. 161–174.

Miller, C.F., and Mittlefehldt, D.W., 1982, Depletion of light rare-earth elements in felsic magmas: Geology, v. 10, p. 129–133.

Pallister, J.S., Hoblitt, R.P, Crandell, D.R., and Mullineaux, D.R., 1992, Mount St. Helens a decade after the 1980 eruptions—Magmatic models and a revised hazards assessment: Bulletin of Volcanology, v. 54, p. 126–146.

Pearce, J.A., Harris, N.B.W., and Tindle, A.G., 1984, Trace element discrimination diagrams for the tectonic interpretation of granitic rocks: Journal of Petrology, v. 25, p. 956–983.

Sawka, W.N., Chappell, B.W., and Kistler, R.W., 1990, Granitoid compositional zoning by side-wall boundary layer differentiation—Evidence from the Palisade Crest Intrusive Suite, central Sierra Nevada, California: Journal of Petrology, v. 31, p. 519–553.

Sawyer, D.A., and Sargent, K.A., 1989, Petrologic evolution of divergent peralkaline magmas from the Silent Canyon caldera complex, southwestern Nevada volcanic field: Journal of Geophysical Research, v. 94, p. 6021–6040.

Sillitoe, R.H., 1973, The tops and bottoms of porphyry copper deposits: Economic Geology, v. 68, p. 799–815.

Smith, R.L., 1979, Ash-flow magmatism: Geological Society of America Special Paper 180, p. 5–27.

Stewart, J.H., and Carlson, J.E., 1978, Geologic map of Nevada: U.S. Geological Survey, scale 1:500,000.

Swanson, D.A., Dzurisin, D., Holcomb, R.T., Iwatsubo, E.Y., Chadwick, W.W., Casadevall, T.J., Ewert, J.W., and Heliker, C.C., 1987, Growth of the lava dome at Mount St. Helens, Washington (USA) 1981–1983: Geological Society of America Special Paper 212, p. 1–16.

Taggart, J.E., Lindsay, J.R., Scott, B.A., Vivit, D.V., Bartel, A.J., and Stewart, K.C., 1987, Analysis of geologic materials by X-ray fluorescence spectrometry, *in* Baedecker, P.A., ed., Methods for geochemical analysis: U.S. Geological Survey Bulletin 1770, p. E1–E19.

Taylor, W.J., and Bartley, J.M., 1988, Stratigraphy and structure in the North Pahroc and eastern Seaman Ranges, *in* Weide, D.L., and Faber, M.W., eds., Cordilleran Section fieldtrip guidebook: Geological Society of America, p. 5–6.

Taylor, W.J., Bartley, J.M., Lux, D.R., and Axen, G.J., 1989, Timing of Tertiary extension in the Railroad Valley–Pioche transect, Nevada—Constraints from $^{40}Ar/^{39}Ar$ ages of volcanic rocks: Journal of Geophysical Research, v. 94, p. 7757–7774.

Thompson, R.N., Morrison, M.A., Dickin, A.P., Hendry, G.L., 1983, Continental flood basalts...Arachnids rule OK?, *in* Continental flood basalts and xenoliths: Cheshire, England, Shiva Publishing, p. 158–185.

Tschanz, C.M., and Pampeyan, E.H., 1961, Preliminary geologic map of Lincoln County, Nevada: U.S. Geological Survey Mineral Investigations Field Studies Map MF–206, scale 1:200,000.

———1970, Geology and mineral deposits of Lincoln County, Nevada: Nevada Bureau of Mines and Geology Bulletin 73, 188 p.

Whitney, J.A., 1988, The origin of granite—The role and source of water in the evolution of granitic magmas: Geological Society of America Bulletin, v. 100, p. 1886–1897.

Williams, P.L., 1967, Stratigraphy and petrography of the Quichapa Group, southwestern Utah and southeastern Nevada: Seattle, University of Washington, Ph.D. thesis, 139 p.

Wood, D.A., Joron, J.-L., and Treuil, M., 1979, A re-appraisal of the use of trace elements to classify and discriminate between magma series erupted in different tectonic settings: Earth and Planetary Science Letters, v. 45, p. 326–336.

Published in the Central Region, Denver, Colorado
Manuscript approved for publication December 18, 1992
Edited by Judith Stoeser
Type composed by Shelly A. Fields
Graphics prepared by Edward du Bray

☆U.S. GOVERNMENT PRINTING OFFICE: 1993-774-049/66047

SELECTED SERIES OF U.S. GEOLOGICAL SURVEY PUBLICATIONS

Periodicals

Earthquakes & Volcanoes (issued bimonthly).
Preliminary Determination of Epicenters (issued monthly).

Technical Books and Reports

Professional Papers are mainly comprehensive scientific reports of wide and lasting interest and importance to professional scientists and engineers. Included are reports on the results of resource studies and of topographic, hydrologic, and geologic investigations. They also include collections of related papers addressing different aspects of a single scientific topic.

Bulletins contain significant data and interpretations that are of lasting scientific interest but are generally more limited in scope or geographic coverage than Professional Papers. They include the results of resource studies and of geologic and topographic investigations; as well as collections of short papers related to a specific topic.

Water-Supply Papers are comprehensive reports that present significant interpretive results of hydrologic investigations of wide interest to professional geologists, hydrologists, and engineers. The series covers investigations in all phases of hydrology, including hydrology, availability of water, quality of water, and use of water.

Circulars present administrative information or important scientific information of wide popular interest in a format designed for distribution at no cost to the public. Information is usually of short-term interest.

Water-Resources Investigations Reports are papers of an interpretive nature made available to the public outside the formal USGS publications series. Copies are reproduced on request unlike formal USGS publications, and they are also available for public inspection at depositories indicated in USGS catalogs.

Open-File Reports include unpublished manuscript reports, maps, and other material that are made available for public consultation at depositories. They are a nonpermanent form of publication that maybe cited in other publications as sources of information.

Maps

Geologic Quadrangle Maps are multicolor geologic maps on topographic bases in 7 1/2- or 15-minute quadrangle formats (scales mainly 1:24,000 or 1:62,500) showing bedrock, surficial, or engineering geology. Maps generally include brief texts; some maps include structure and columnar sections only.

Geophysical Investigations Maps are on topographic or planimetric bases at various scales, they show results of surveys using geophysical techniques, such as gravity, magnetic, seismic, or radioactivity, which reflect subsurface structures that are of economic or geologic significance. Many maps include correlations with the geology.

Miscellaneous Investigations Series Maps are on planimetric or topographic bases of regular and irregular areas at various scales; they present a wide variety of format and subject matter. The series also includes 7 1/2-minute quadrangle photogeologic maps on planimetric bases which show geology as interpreted from aerial photographs. The series also includes maps of Mars and the Moon.

Coal Investigations Maps are geologic maps on topographic or planimetric bases at various scales showing bedrock or surficial geology, stratigraphy, and structural relations in certain coal-resource areas.

Oil and Gas Investigations Charts show stratigraphic information for certain oil and gas fields and other areas having petroleum potential.

Miscellaneous Field Studies Maps are multicolor or black-and-white maps on topographic or planimetric bases on quadrangle or irregular areas at various scales. Pre-1971 maps show bedrock geology in relation to specific mining or mineral-deposit problems; post-1971 maps are primarily black-and-white maps on various subjects such as environmental studies or wilderness mineral investigations.

Hydrologic Investigations Atlases are multicolored or black-and-white maps on topographic or planimetric bases presenting a wide range of geohydrologic data of both regular and irregular areas; the principal scale is 1:24,000, and regional studies are at 1:250,000 scale or smaller.

Catalogs

Permanent catalogs, as well as some others, giving comprehensive listings of U.S. Geological Survey publications are available under the conditions indicated below from USGS Map Distribution, Box 25286, Building 810, Denver Federal Center, Denver, CO 80225. (See latest Price and Availability List.)

"Publications of the Geological Survey, 1879-1961" may be purchased by mail and over the counter in paperback book form and as a set microfiche.

"Publications of the Geological Survey, 1962-1970" may be purchased by mail and over the counter in paperback book form and as a set of microfiche.

"Publications of the U.S. Geological Survey, 1971-1981" may be purchased by mail and over the counter in paperback book form (two volumes, publications listing and index) and as a set of microfiche.

Supplements for 1982, 1983, 1984, 1985, 1986, and for subsequent years since the last permanent catalog may be purchased by mail and over the counter in paperback book form.

State catalogs, "List of U.S. Geological Survey Geologic and Water-Supply Reports and Maps For (State)," may be purchased by mail and over the counter in paperback booklet form only.

"Price and Availability List of U.S. Geological Survey Publications," issued annually, is available free of charge in paperback booklet form only.

Selected copies of a monthly catalog "New Publications of the U.S. Geological Survey" is available free of charge by mail or may be obtained over the counter in paperback booklet form only. Those wishing a free subscription to the monthly catalog "New Publications of the U.S. Geological Survey" should write to the U.S. Geological Survey, 582 National Center, Reston, VA 22092.

Note.–Prices of Government publications listed in older catalogs, announcements, and publications may be incorrect. Therefore, the prices charged may differ from the prices in catalogs, announcements, and publications.